Two-fluid model for a rotating trapped Fermi gas in the BCS phase

Michael Urban
Institut de Physique Nucléaire, F-91406 Orsay Cédex, France
(Received 5 November 2004; published 8 March 2005)

We investigate the dynamical properties of a superfluid gas of trapped fermionic atoms in the BCS phase. As a simple example we consider the reaction of the gas to a slow rotation of the trap. It is shown that the currents generated by the rotation can be understood within a two-fluid model similar to the one used in the theory of superconductors, but with a position-dependent ratio of normal and superfluid densities. The rather general result of this paper is that already at very low temperatures, far below the critical one, an important normal-fluid component appears in the outer regions of the gas. This renders the experimental observation of superfluidity effects more difficult and indicates that reliable theoretical predictions concerning other dynamical properties, like the frequencies of collective modes, can only be made by taking into account temperature effects.

DOI: 10.1103/PhysRevA.71.033611 PACS number(s): 03.75.Kk, 03.75.Ss, 67.40.Bz

I. INTRODUCTION

In the last few months, experiments with trapped fermionic ^{6}Li atoms made great progress. The fact that by using the Feshbach resonance the Fermi gas can be transformed into a Bose-Einstein condensate (BEC) of molecules, which can be cooled by evaporative cooling and afterward transformed back into a Fermi gas, allows one to reach extremely low temperatures of the order of $0.03T_F$ [1], where $T_F = k_B\epsilon_F$ is the Fermi temperature. This allows, among other things, a detailed study of the BEC-BCS crossover. In particular, a temperature of $0.03T_F$ should even be low enough to realize the BCS phase which is characterized by the condition $\Delta \ll \epsilon_F$, where Δ denotes the pairing gap.

However, at present it is not very clear how the transition to the BCS phase could be detected. While several observables related to collective oscillations (e.g., breathing modes) of the system have been investigated [1,2], the most unambiguous signatures of the superfluid BCS phase seem to be those that concern the rotational properties of the system [3]. For instance, the moment of inertia of a slowly rotating Fermi gas was proposed to be a suitable observable for the detection of the BCS transition [4]. It should be mentioned that at present most of the theoretical predictions concerning possible experimental signatures of the BCS phase (e.g., [3,5–8]) neglect temperature effects as well as possible deviations from hydrodynamic behavior due to the discrete level spectrum in the trap.

In a previous article [9] we calculated the moment of inertia of a superfluid atomic Fermi gas in a slowly rotating trap at finite temperature. There it turned out that the irrotational flow, which is characteristic for superfluidity, is realized only in the limit when the gap Δ is very large compared with the temperature T and the level spacing $\hbar\omega$ of the trap. In all other cases, the velocity field has both rotational and irrotational components. For example, if the level spacing $\hbar\omega$ is comparable with Δ, the current has a strong rotational component even at zero temperature. On the other hand, at nonvanishing temperature T, a certain fraction of the Cooper pairs is broken by thermal excitations. This leads to the well-known effect that the system behaves like a mixture of normal and superfluid components [10–12]. Under rotation, the former behaves like a rigid body, while the latter can only have an irrotational velocity field.

However, in the calculation of Ref. [9] the gap $\Delta(\mathbf{r})$ has been replaced by a constant Δ corresponding to the average diagonal matrix element of $\Delta(\mathbf{r})$ at the Fermi surface. While this averaging procedure seems to be justified in cases where only one oscillator shell participates in the pairing (intrashell pairing, $\Delta < \hbar\omega$), it is not well suited for the strong pairing regime ($\Delta > \hbar\omega$), where the properties of the system can be described locally and depend on $\mathbf{r}$ via the spatial dependence of $\Delta(\mathbf{r})$ [13]. In particular, the normal and superfluid fractions of the density, ρ_n/ρ and ρ_s/ρ, should depend on $\mathbf{r}$. To our knowledge this fact has not been taken into account in the existing published literature. The author recently learned that the $\mathbf{r}$ dependence of ρ_n and ρ_s has been considered by Nygaard in Ref. [14], but there the derivation follows a completely different method and no numerical results are presented.

In this article, we will concentrate on the $\hbar \to 0$ limit, i.e., we will neglect the quantum effect which is responsible for the rotational component of the velocity field at zero temperature. Anyway, if the system is sufficiently large and if the temperature is not extremely low, this quantum effect becomes much smaller than the effect resulting from the thermally created normal component of the system. The important point is that we will now take into account the $\mathbf{r}$ dependence of the gap. In addition, we will not rely on the simplification made in our previous work that the full potential (trap + mean field) is approximately harmonic.

II. DERIVATIONS

In this section we will derive expressions for the normal and superfluid parts of the current density in a slowly rotating superfluid Fermi gas. This decomposition of the current will allow us to extract the normal and superfluid fractions of the total density of the system. Let us briefly summarize some basic formulas (for more explanations and details, see

Ref. [9]). We assume that equal numbers of atoms in two spin states are trapped in a harmonic potential,

$$V_{\rm trap}(\mathbf{r}) = \sum_{i=xyz} \frac{m\omega_i^2}{2} r_i^2. \tag{1}$$

The cigar-shaped form of the traps used in current experiments corresponds to $\omega_z \ll \omega_x = \omega_y$. However, in order to force the system to rotate around the long axis, one has to break the axial symmetry, e.g., by using a rotating laser beam as "spoon." We will model this by taking $\omega_x \neq \omega_y$. The mean-field single-particle Hamiltonian minus the chemical potential reads

$$\hat{h}_0 = \frac{\hat{\mathbf{p}}^2}{2m} + V_{\rm trap}(\mathbf{r}) + g\ \rho(\mathbf{r}) - \mu, \tag{2}$$

the coupling constant $g = 4\pi\hbar^2 a/m$ being proportional to the atom-atom scattering length $a < 0$, and $\rho(\mathbf{r})$ being the density per spin state. The order parameter in equilibrium is denoted $\Delta_0(\mathbf{r})$. Note that we will rely on the validity of mean-field theory throughout this article. This is the reason why we have to restrict ourselves to the BCS phase. In the BEC-BCS crossover region, it would be necessary to include quantum and thermal fluctuations [15].

Now we want to describe what happens if the trap is slowly rotating around the z axis with a rotation frequency $\mathbf{\Omega} = \Omega \mathbf{e}_z$. This is most easily done in the rotating reference frame. Then we still have a static problem, but the Hamiltonian receives the additional term

$$\hat{h}_1 = -\Omega \hat{L}_z = -(\mathbf{\Omega} \times \mathbf{r}) \cdot \hat{\mathbf{p}}, \tag{3}$$

which we will treat as a small perturbation. Because of this term, the order parameter $\Delta(\mathbf{r})$ receives a phase $\exp[-2i\phi(\mathbf{r})]$. The explicit form of $\phi(\mathbf{r})$ is unknown for the moment and will be determined below. It is convenient to eliminate this phase by a gauge transformation, multiplying all single-particle wave functions by $\exp[i\phi(\mathbf{r})]$. In this way the gauge-transformed gap $\tilde{\Delta}(\mathbf{r})$ stays real, which in the case of a slow rotation implies that $\tilde{\Delta}$ does not change at all,[1] i.e., $\tilde{\Delta} = \Delta_0$. On the other hand, this gauge transformation changes the momentum operator according to

$$\hat{\tilde{\mathbf{p}}} = \hat{\mathbf{p}} - \hbar\, \boldsymbol{\nabla}\, \phi(\mathbf{r}). \tag{4}$$

Hence, the price to pay for the real gap is an additional term in the Hamiltonian. To linear order in the rotation frequency the new perturbation Hamiltonian reads

$$\hat{\tilde{h}}_1 = -\Omega \hat{L}_z - \frac{\hbar}{2m}\{\hat{\mathbf{p}} \cdot [\boldsymbol{\nabla}\phi(\mathbf{r})] + [\boldsymbol{\nabla}\phi(\mathbf{r})] \cdot \hat{\mathbf{p}}\}. \tag{5}$$

In order to describe the system semiclassically, we make use of the Wigner-Kirkwood expansion. To that end we denote the Wigner transforms of $\hat{h}_0, \hat{\tilde{h}}_1$, etc., by $h_0(\mathbf{r},\mathbf{p}), \tilde{h}_1(\mathbf{r},\mathbf{p})$, etc. We need also the Wigner transforms of the normal and abnormal density matrices in equilibrium, $\rho_0(\mathbf{r},\mathbf{p})$ and $\kappa_0(\mathbf{r},\mathbf{p})$, as well as their deviations from equilibrium, $\tilde{\rho}_1(\mathbf{r},\mathbf{p})$ and $\tilde{\kappa}_1(\mathbf{r},\mathbf{p})$. (For the sake of brevity, we will occasionally omit the arguments $\mathbf{r}$ and $\mathbf{p}$ if there is no risk of confusion.) Furthermore we introduce the Poisson brackets of two phase-space functions

$$\{f,g\} = \sum_{i=x,y,z} \left(\frac{\partial f}{\partial r_i}\frac{\partial g}{\partial p_i} - \frac{\partial f}{\partial p_i}\frac{\partial g}{\partial r_i} \right). \tag{6}$$

Using the notations defined above, the terms linear in Ω of the Hartree-Fock-Bogoliubov (HFB) or Bogoliubov–de Gennes equations up to linear order in $\hbar$ can be written as

$$i\hbar\{h_0,\tilde{\rho}_1\} + 2\Delta_0\tilde{\kappa}_1 = -i\hbar\{\tilde{h}_1,\rho_0\}, \tag{7}$$

$$i\hbar\{\Delta_0,\tilde{\rho}_1\} - 2h_0\tilde{\kappa}_1 = i\hbar\{\tilde{h}_1,\tilde{\kappa}_0\}. \tag{8}$$

These are exactly Eqs. (84) and (85) of Ref. [9]. The main point of the present article concerns the solution of this system of equations in the case of an $\mathbf{r}$-dependent gap $\Delta_0(\mathbf{r})$.

First we eliminate $\tilde{\kappa}_1$ by multiplying Eq. (7) by h_0 and Eq. (8) by Δ_0 and adding up the two resulting equations. Using the chain and product rules of differentiation, we then obtain

$$\tfrac{1}{2}\{E^2,\tilde{\rho}_1\} = -h_0\{\tilde{h}_1,\rho_0\} + \Delta_0\{\tilde{h}_1,\kappa_0\}, \tag{9}$$

where $E^2(\mathbf{r},\mathbf{p}) = h_0^2(\mathbf{r},\mathbf{p}) + \Delta_0^2(\mathbf{r})$. To proceed further, we express ρ_0 and κ_0 in terms of h_0 and Δ_0. Within the Thomas-Fermi (TF) or local-density approximation, these relations read

$$\rho_0(\mathbf{r},\mathbf{p}) = \frac{1}{2} - \frac{h_0(\mathbf{r},\mathbf{p})}{2E(\mathbf{r},\mathbf{p})}[1 - 2f(E(\mathbf{r},\mathbf{p}))], \tag{10}$$

$$\kappa_0(\mathbf{r},\mathbf{p}) = \frac{\Delta_0(\mathbf{r})}{2E(\mathbf{r},\mathbf{p})}[1 - 2f(E(\mathbf{r},\mathbf{p}))], \tag{11}$$

where $f(E) = 1/[\exp(E/k_BT) + 1]$ denotes the Fermi function. Although Eqs. (10) and (11) are the solutions of the $\hbar \to 0$ limit of the HFB equations, they are valid up to linear order in $\hbar$ [16] and therefore consistent with Eqs. (7) and (8). Inserting Eqs. (10) and (11) into Eq. (9), we obtain, again after repeated use of chain and product rules of differentiation, the following simple equation:

$$\frac{1}{2}\{E^2,\tilde{\rho}_1\} = \frac{1}{2}\left\{ E^2, \tilde{h}_1 \frac{df}{dE} \right\}. \tag{12}$$

It is evident that this equation is solved by

$$\tilde{\rho}_1 = \tilde{h}_1 \frac{df}{dE}. \tag{13}$$

However, before this solution can be used, the gauge transformation that has been introduced in order to make the gap real must be inverted:

$$\rho(\mathbf{r},\mathbf{p}) = \tilde{\rho}[\mathbf{r},\mathbf{p} + \hbar\, \boldsymbol{\nabla}\, \phi(\mathbf{r})]. \tag{14}$$

To linear order in Ω, this can also be written as

$$\rho(\mathbf{r},\mathbf{p}) = \rho_0[\mathbf{r},\mathbf{p} + \hbar\, \boldsymbol{\nabla}\, \phi(\mathbf{r})] + \tilde{\rho}_1(\mathbf{r},\mathbf{p}) \tag{15}$$

[1] Since the magnitude of Δ cannot depend on the sign of Ω, its change must be at least of the order Ω^2.

$$= \rho_0[\mathbf{r}, \mathbf{p} + \hbar \nabla \phi(\mathbf{r})] - \left(\mathbf{\Omega} \times \mathbf{r} + \frac{\hbar}{m} \nabla \phi(\mathbf{r}) \right) \cdot \mathbf{p} \left. \frac{df}{dE} \right|_{E(\mathbf{r},\mathbf{p})}. \quad (16)$$

The last line has been obtained with the help of Eqs. (5) and (13).

The next step consists in calculating the corresponding current density per spin state,

$$\mathbf{j}(\mathbf{r}) = \int \frac{d^3p}{(2\pi\hbar)^3} \frac{\mathbf{p}}{m} \rho(\mathbf{r}, \mathbf{p}). \quad (17)$$

Using the explicit expression for $\rho(\mathbf{r}, \mathbf{p})$ given above, one easily obtains

$$\mathbf{j}(\mathbf{r}) = -\rho_0(\mathbf{r}) \frac{\hbar}{m} \nabla \phi(\mathbf{r}) - \left(\mathbf{\Omega} \times \mathbf{r} + \frac{\hbar}{m} \nabla \phi(\mathbf{r}) \right) \times \int_0^\infty \frac{dp}{6\pi^2\hbar^3} \frac{p^4}{m} \left. \frac{df}{dE} \right|_{E(\mathbf{r},p)}, \quad (18)$$

with

$$\rho_0(\mathbf{r}) = \int \frac{d^3p}{(2\pi\hbar)^3} \rho_0(\mathbf{r}, \mathbf{p}). \quad (19)$$

The current density can therefore be written in a more suggestive way in terms of normal and superfluid densities $\rho_n(\mathbf{r})$ and $\rho_s(\mathbf{r})$,

$$\mathbf{j}(\mathbf{r}) = \rho_n(\mathbf{r}) \mathbf{\Omega} \times \mathbf{r} - \rho_s(\mathbf{r}) \frac{\hbar}{m} \nabla \phi(\mathbf{r}), \quad (20)$$

if the normal and superfluid densities are defined according to the textbook result (Ref. [17], p. 459) as

$$\rho_n(\mathbf{r}) = \rho_0(\mathbf{r}) - \rho_s(\mathbf{r}) = -\int_0^\infty \frac{dp}{6\pi^2\hbar^3} \frac{p^4}{m} \left. \frac{df}{dE} \right|_{E(\mathbf{r},p)}. \quad (21)$$

In the BCS limit, i.e., if $\Delta_0(\mathbf{r}) \ll \epsilon_F(\mathbf{r})$, where $\epsilon_F(\mathbf{r}) = \mu - V_{\text{trap}}(\mathbf{r}) - g\rho_0(\mathbf{r})$ denotes the local Fermi energy, the ratio $\rho_n(\mathbf{r})/\rho_0(\mathbf{r})$ becomes a function of only one dimensionless argument $T/T_c(\mathbf{r})$, where $T_c(\mathbf{r}) = 0.57\Delta_0(\mathbf{r}; T=0)$ denotes the local critical temperature (the existence of a local critical temperature is an artifact of the TF approximation; see the discussion in Sec. III). This function, as well as the temperature dependence of the ratio $\Delta_0(\mathbf{r})/\Delta_0(\mathbf{r}; T=0)$, is shown in Fig. 1.

Up to now, the phase $\phi(\mathbf{r})$, which determines the velocity of the superfluid component, is completely unknown. In Ref. [9], this phase was determined by calculating $\tilde{\Delta}_1$ from $\tilde{\kappa}_1$ and imposing the condition $\tilde{\Delta}_1 = 0$. Then it was shown that with this choice the continuity equation for the current was satisfied. Here we will adopt another method which is commonly used in the literature [11] and which consists in using the continuity equation. In the rotating frame the latter reads

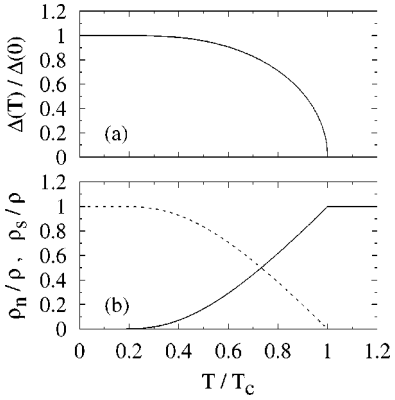

FIG. 1. (a) Temperature dependence of the gap normalized to its value at zero temperature $[\Delta(0) = 1.76T_c]$. (b) Temperature dependence of the normal (solid line) and superfluid (dashed line) fractions of the superfluid system in the limit of weak pairing ($\Delta \ll \epsilon_F$). These relations hold locally, if T_c is interpreted as the local critical temperature, defined by $T_c(\mathbf{r}) = 0.57\Delta(\mathbf{r}; T=0)$.

$$\nabla \cdot \mathbf{j}(\mathbf{r}) + \dot{\rho}(\mathbf{r}) - (\mathbf{\Omega} \times \mathbf{r}) \cdot \nabla \rho(\mathbf{r}) = 0, \quad (22)$$

where $\dot{\rho}(\mathbf{r}) = 0$ in our case of a stationary rotation and $\rho(\mathbf{r}) = \rho_0(\mathbf{r})$ up to linear order in Ω. Taking the divergence of Eq. (20), one can see that the normal-fluid component drops out and it remains a continuity equation for the superfluid component:

$$-\frac{\hbar}{m} \nabla \cdot [\rho_s(\mathbf{r}) \nabla \phi(\mathbf{r})] - (\mathbf{\Omega} \times \mathbf{r}) \cdot \nabla \rho_s(\mathbf{r}) = 0. \quad (23)$$

In the case of a deformed harmonic trapping potential, this equation can be solved analytically. To see this, remember that within the TF approximation the density $\rho_0(\mathbf{r})$ and the gap $\Delta_0(\mathbf{r})$, and consequently also the superfluid density ρ_s, depend on $\mathbf{r}$ only via the local chemical potential $\mu_{\text{loc}}(\mathbf{r}) = \mu - V_{\text{trap}}(\mathbf{r})$, i.e., $\rho_s(\mathbf{r}) = \rho_s[\mu - V_{\text{trap}}(\mathbf{r})]$. Hence Eq. (23) can be written as

$$\left. \frac{d\rho_s}{d\mu_{\text{loc}}} \right|_{\mu - V_{\text{trap}}(\mathbf{r})} [\nabla V_{\text{trap}}(\mathbf{r})] \cdot \left(\frac{\hbar}{m} \nabla \phi(\mathbf{r}) + \mathbf{\Omega} \times \mathbf{r} \right) - \frac{\hbar}{m} \rho_s(\mathbf{r}) \nabla^2 \phi(\mathbf{r}) = 0. \quad (24)$$

In the special case of the harmonic potential (1), it can readily be shown that this equation has the same solution as in the simple case of constant Δ_0 studied in Ref. [9],

$$\phi(\mathbf{r}) = \frac{m}{\hbar} \frac{\omega_x^2 - \omega_y^2}{\omega_x^2 + \omega_y^2} \Omega r_x r_y, \quad (25)$$

since this solution is independent of the form of $\rho_s(\mu)$. The current density per spin state, $\mathbf{j}(\mathbf{r})$, is therefore given by

$$\mathbf{j}(\mathbf{r}) = \rho_n(\mathbf{r}) \mathbf{\Omega} \times \mathbf{r} - \rho_s(\mathbf{r}) \frac{\omega_x^2 - \omega_y^2}{\omega_x^2 + \omega_y^2} \Omega \nabla (r_x r_y). \quad (26)$$

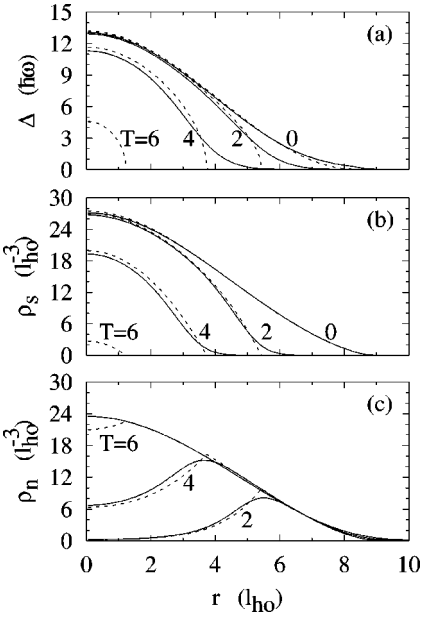

FIG. 2. (a) Gap $\overline{\Delta_0}(r)$, (b) superfluid density $\overline{\rho_s}(r)$, and (c) normal-fluid density $\overline{\rho_n}(r)$ as a function of the distance r from the center of the spherical trap with frequency $\overline{\omega}$ for several temperatures: $T=(0,2,4,6)\hbar\overline{\omega}/k_B$. For convenience, all quantities are given in harmonic oscillator units, i.e., r in $l_{\rm ho}=\sqrt{\hbar/m\overline{\omega}}$, $\overline{\Delta_0}$ in $\hbar\overline{\omega}$, $\overline{\rho_s}$ and $\overline{\rho_n}$ in $l_{\rm ho}^{-3}$. The number of atoms is 36 000, their interaction strength is set to $g=-\hbar^2 l_{\rm ho}/m$. This choice of parameters allows us to compare the TF results (dashed lines) with results obtained from a numerical solution of the full HFB equations (solid lines). In (a) and (b), the solid lines for $T=6\,\hbar\overline{\omega}/k_B$ are not visible since in this case $\overline{\Delta_0}$ and $\overline{\rho_s}$ are equal to zero.

III. NUMERICAL RESULTS

As mentioned above, $\rho_0(\mathbf{r})$ and $\Delta_0(\mathbf{r})$ [and consequently $\rho_s(\mathbf{r})$ and $\rho_n(\mathbf{r})$] depend on $\mathbf{r}$ only via the local chemical potential. Therefore it is sufficient to perform the TF calculation for a spherical trap with the geometrically averaged trapping frequency $\overline{\omega}=(\omega_x\omega_y\omega_z)^{1/3}$. In this spherical trap, of course, the density $\overline{\rho_0}$, gap $\overline{\Delta_0}$, etc., depend only on the distance from the center, i.e., $\overline{\rho_0}(\mathbf{r})=\overline{\rho_0}(r)$, etc. (quantities related to the spherical trap will be marked by an overbar bar). The corresponding quantities in the deformed trap can then be obtained from

$$\rho_0(\mathbf{r}) = \overline{\rho_0}\left(\frac{1}{\overline{\omega}}\sqrt{\omega_x^2 r_x^2+\omega_y^2 r_y^2+\omega_z^2 r_z^2}\right) \tag{27}$$

and analogously for $\Delta_0(\mathbf{r}), \rho_s(\mathbf{r})$, etc. Note, however, that all this is true only within the TF approximation.

In Fig. 2 we show the normal and superfluid densities per spin state ($\overline{\rho_n}$ and $\overline{\rho_s}$) and the gap $\overline{\Delta_0}$ in the spherical trap for different temperatures. The dashed lines correspond to the TF ($\hbar\to 0$) results. For the solid lines the gap $\overline{\Delta_0}$ has been obtained by solving numerically the HFB equations [18,19], but the densities ρ_n and ρ_s have again been obtained from Eq. (21).[2]

In order to make the comparison between the gaps $\overline{\Delta_0}$ calculated within the TF approximation and by solving the full HFB equations, we had to choose a rather moderate number of particles, $N=36\,000$, for which the HFB calculation is feasible. Unfortunately, for realistic numbers of particles, like $N=4\times 10^5$ as quoted in Ref. [1], we are not able to solve the HFB equations numerically. Of course, this limitation does not concern the calculations done within the TF approximation. If we had not been interested in the comparison between the results obtained with the HFB and TF gaps, we could have shown the TF results for arbitrarily large numbers of particles. We emphasize that even for much larger numbers of particles the qualitative behavior of the TF results remains unchanged, provided that the coupling constant g is tuned such that the condition $\Delta \ll \epsilon_F$ (BCS condition) remains satisfied[3] and the temperatures are scaled with respect to the critical temperature.

Before discussing the normal and superfluid densities, let us briefly comment on the temperature dependence of the gap, Fig. 2(a). It can be seen that at zero temperature the HFB and TF gaps are in very good agreement. At nonzero temperature, however, the TF gap becomes exactly zero beyond a certain radius, because of the fact that within the TF approximation to each point $\mathbf{r}$ corresponds a critical temperature $T_c(\mathbf{r})$ depending on the local chemical potential $\mu_{\rm loc}(\mathbf{r})$ at that point. With increasing temperature, this radius becomes smaller and smaller, and finally, at $T=T_c(\mathbf{r}=\mathbf{0})$ the gap vanishes everywhere. The temperature $T_c(\mathbf{r}=\mathbf{0})$ has therefore been identified with the critical temperature $T_{c,\rm TF}$ of the system within the TF approximation [20]. This behavior is different from that obtained within the HFB calculation, where the critical temperature T_c is a global quantity, i.e., for $T<T_c$ the gap is nonzero everywhere (although extremely small at large r). This global critical temperature $T_{c,\rm HFB}$ is lower than $T_{c,\rm TF}$ [19,21]: for the present parameters, we find $T_{c,\rm HFB}\approx 5.5\hbar\overline{\omega}$ and $T_{c,\rm TF}\approx 6.2\hbar\overline{\omega}$. This explains why in Fig. 2(a) the TF gap at $T=6\hbar\overline{\omega}$ is nonzero at the center, whereas the HFB gap is zero everywhere at this temperature.

Now we turn to the superfluid and normal densities shown in Figs. 2(b) and 2(c), respectively. At zero temperature, the trapped Fermi gas is completely superfluid, i.e., $\overline{\rho_s}=\overline{\rho_0}$ and $\overline{\rho_n}=0$. At low but nonvanishing temperature ($T=2\hbar\overline{\omega}\approx 0.36T_{c,\rm HFB}$) a normal-fluid component appears near the surface, since there the gap is smallest and consequently the Cooper pairs are most easily broken by thermal excitations. If the temperature increases further ($T=4\hbar\overline{\omega}\approx 0.72T_{c,\rm HFB}$), the normal-fluid component starts to extend over the whole volume, and finally, slightly above the critical temperature ($T=6\hbar\overline{\omega}$) the superfluid component vanishes completely

[2] In Ref. [14] a formula is given to calculate ρ_n and ρ_s without resorting to any semiclassical approximation. For the parameters used here, this formula gives results which are very close to those obtained from Eq. (21).

[3] At zero temperature and at the center of the trap we have with our choice of parameters $\Delta\approx 0.2\epsilon_F$, i.e., we are already close to the BCS-BEC crossover region.

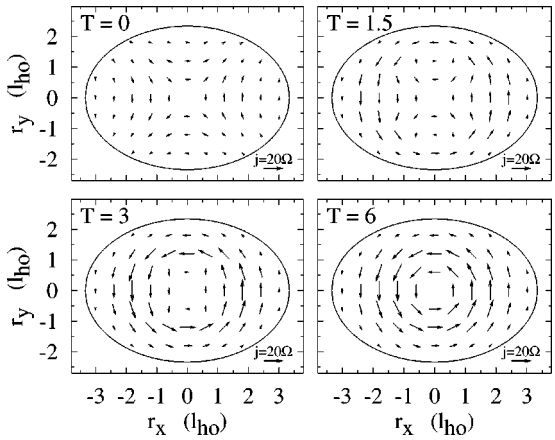

FIG. 3. Current density divided by the angular velocity of the rotation, $\mathbf{j}(\mathbf{r})/\Omega$, in the xy plane ($r_z=0$) of a trap with $\omega_x/\omega_y=0.7$ and $\omega_z/\omega_r=0.03$ ($\omega_r=\sqrt{\omega_x\omega_y}$) at four different temperatures. The remaining parameters are the same as in Fig. 2. The length of the arrow displayed in the lower right corner of each figure corresponds to a current density of $j=20\Omega/l_{\mathrm{ho}}^2$. The coordinates r_x and r_y are given in units of l_{ho} and the temperatures in units of $\hbar\bar{\omega}/k_B$.

(solid lines). Within the TF approximation (dashed lines), there is still a small superfluid region surviving near the center of the trap at $T=6\hbar\bar{\omega}$ because of $T_{c,\mathrm{TF}}\approx 6.2\hbar\bar{\omega}$. However, apart from this point, one can say that in general for $\bar{\rho}_n$ and $\bar{\rho}_s$ the agreement between TF and HFB is reasonable and better than for the gap $\bar{\Delta}_0$ itself. The reason why the agreement between TF and HFB is better for $\bar{\rho}_n$ and $\bar{\rho}_s$ than for $\bar{\Delta}_0$ is that near the critical temperature the temperature dependence of ρ_s/ρ is much weaker than that of $\Delta/\Delta(T=0)$ (see Fig. 1).

Using the spherical density profiles and Eqs. (26) and (27), we can immediately calculate the current distribution $\mathbf{j}(\mathbf{r})$. In Fig. 3 we show the current in the xy plane ($r_z=0$) for a deviation from axial symmetry of $\omega_x/\omega_y=0.7$ at several temperatures. (For the cases shown, the current densities obtained from the HFB and TF density profiles are indistinguishable within the resolution of the plot.) At zero temperature, the current is irrotational and rather weak (it vanishes in the limit of axial symmetry, $\omega_x=\omega_y$). In the surface region the current reaches its ordinary (rigid-body) form already at $T=1.5\hbar\bar{\omega}\approx 0.27T_c$. At $T=3\hbar\bar{\omega}\approx 0.54T_c$ the current shows almost everywhere the rigid-body behavior, only near the center is it still a little bit weaker than in the normal phase, $T=6\hbar\bar{\omega}$.

Let us now look at the temperature dependence of the moment of inertia Θ, which is defined as

$$\Theta=\frac{\langle\hat{L}_z\rangle}{\Omega}=\frac{2m}{\Omega}\int d^3r[r_x j_y(\mathbf{r})-r_y j_x(\mathbf{r})]. \tag{28}$$

The factor of 2 is a consequence of our convention that $\mathbf{j}$ denotes the current density per spin state. Using again Eqs. (27) and (26), we can express the moment of inertia in terms of the density profile in the corresponding spherical trap as a simple radial integral:

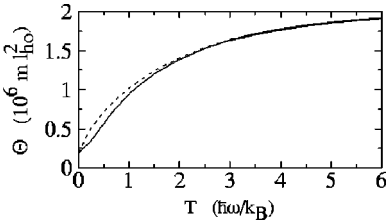

FIG. 4. Moment of inertia Θ of a trapped Fermi gas as function of temperature. The parameters are the same as in Figs. 2 and 3. The moment of inertia and the temperature are given in harmonic oscillator units, i.e., Θ in ml_{ho}^2 and T in $\hbar\bar{\omega}/k_B$. The transition temperature to the BCS phase lies at approximately $5.5\hbar\bar{\omega}$. The solid line has been obtained by performing a full HFB calculation for $\bar{\rho}_0(r)$ and $\bar{\Delta}_0(r)$, while for the dashed line the TF results have been used.

$$\Theta=\frac{8\pi m}{3}\left(\frac{\bar{\omega}^2}{\omega_x^2}+\frac{\bar{\omega}^2}{\omega_y^2}\right)\int_0^\infty dr\, r^4\left[\bar{\rho}_n(r)+\left(\frac{\omega_x^2-\omega_y^2}{\omega_x^2+\omega_y^2}\right)^2\bar{\rho}_s(r)\right]. \tag{29}$$

In Fig. 4 we show the moment of inertia for the same set of parameters that were already used in Figs. 2 and 3 as a function of temperature. The solid line has been calculated by using the HFB density profiles, while the dashed line was obtained from the density profile within TF approximation. One can see that the moment of inertia decreases strongly as the temperature goes to zero. The limiting value at zero temperature is determined by the deformation of the trap in the xy plane,

$$\Theta(T=0)=\left(\frac{\omega_x^2-\omega_y^2}{\omega_x^2+\omega_y^2}\right)^2\Theta_{\mathrm{rigid}}, \tag{30}$$

where Θ_{rigid} denotes the corresponding rigid-body moment of inertia [which can be obtained from Eq. (29) by putting $\bar{\rho}_n=\bar{\rho}_0$ and $\bar{\rho}_s=0$]. In our case of $\omega_x/\omega_y=0.7$, we have $\Theta(T=0)\approx 0.12\Theta_{\mathrm{rigid}}$. Above the critical temperature, the moment of inertia is equal to the rigid-body one. The latter does not stay constant, but it is weakly temperature dependent due to the fact that the radius of the atomic cloud increases with increasing temperature. An important point to notice is that, coming from high temperatures, one does not observe an appreciable change of the moment of inertia until one reaches temperatures far below the critical one. The reason for this effect is that the main contribution to the moment of inertia comes from the outer regions of the trapped gas, where the order parameter becomes small and where consequently the normal-fluid fraction is large even far below T_c. The discrepancy between the HFB (solid line) and TF results (dashed line) below $\approx 2\hbar\bar{\omega}$ can be traced back to the effect that within the TF approximation the gap near the surface vanishes already at very low temperature, such that the normal-fluid fraction near the surface is overestimated within TF.

IV. CONCLUSIONS

In this article we have applied the two-fluid model known from the theory of superconductivity [10–12] to the case of

ultracold trapped fermionic atoms in the BCS phase. In contrast to the usual situation, the ratio of the normal and superfluid densities is explicitly position dependent due to the inhomogeneous trapping potential. Specializing to the case of a slowly rotating system, we have shown that the linear order in $\hbar$ of the linear response equations gives a current which can be decomposed in a natural way into normal and superfluid components. The normal component appears as a consequence of Cooper pairs which are broken by thermal excitations already below the critical temperature T_c. We have shown that especially the outer region of the trapped gas behaves essentially as if it was normal fluid, even far below T_c. Only the central region of the gas keeps its superfluid character up to T_c.

As a consequence, the moment of inertia decreases more slowly than it was previously expected [9] if the temperature is lowered below T_c, i.e., the effects of superfluidity become visible only far below T_c. This important but in a certain sense negative result will apply analogously to other observables which are mainly sensitive to the surface of the system, like, e.g., collective modes. For example, the theory presented here was used in Ref. [22] in order to explain the temperature dependence of the strength of the response function for the so-called "twist mode." There the effect was even more dramatic, since the relevant integral contained an r^6 weight factor instead of r^4 in Eq. (29).

We are therefore convinced that it is not justified to compare the experimentally measured frequencies of collective modes directly with theoretical predictions obtained for zero temperature, as is done in the current literature [1,2]. We rather expect that the temperature dependence is important and can be predicted by generalizing the two-fluid model presented here to the dynamic case, i.e., by performing the Wigner-Kirkwood expansion of the time-dependent HFB equations up to linear order in $\hbar$ [11,23]. This leads to a generalization of the Vlasov equation for the normal phase, which results from the Wigner-Kirkwood expansion of the time-dependent Hartree-Fock equation up to linear order in $\hbar$.

However, one should keep in mind that the Thomas-Fermi approximation for the ground state as well as the Wigner-Kirkwood expansion of the dynamical equations (i.e., the generalized Vlasov equation and the superfluid hydrodynamics to which it reduces in the zero-temperature limit) depend on the assumption $\hbar\omega_i \ll \Delta$ for $i=x,y,z$. Concerning the validity of the Thomas-Fermi approximation for the ground state, the condition $\hbar\omega_i \ll \Delta$ has been inferred from the requirement that the coherence length $\xi=\hbar v_F/\pi\Delta$ (v_F being the Fermi velocity) must be much smaller than the typical length scale of the system, which is approximately given by the Thomas-Fermi radius $R_{\mathrm{TF}}=\sqrt{2\mu/m\omega_i^2}$ [13]. However, it is less evident where the assumption $\hbar\omega_i \ll \Delta$ enters into the description of the dynamics of the system within the generalized Vlasov equation.

To give a specific example, in Ref. [9], quantum corrections to the moment of inertia of higher orders in $\hbar(\omega_x \pm \omega_y)/\Delta$ were discussed. Also in the case of the strength of the twist mode mentioned above, the fully quantum-mechanical ("microscopic") calculation showed deviations from the two-fluid model, especially at very low temperatures. In both cases, the corrections act as if the normal-fluid component of the system was larger than predicted by Eq. (21) and in particular nonvanishing even at zero temperature. In a certain sense the accelerations acting on the Cooper pairs during their motion through the inhomogeneous potential seem to have a similar pair-breaking effect as the thermal excitations which are responsible for the normal-fluid component given by Eq. (21). From a completely different point of view, Eq. (21) is usually derived by looking at the long-wavelength limit ($q\xi \ll 1$) of the current-current correlation function in a homogeneous system [12,17]. In the trapped system, however, the wave vectors must be of the order $q \approx 1/R_{\mathrm{TF}}$, and we recover the condition $\xi \ll R_{\mathrm{TF}}$.

Deviations from superfluid hydrodynamics ($T=0$) or from the two-fluid model ($T>0$), respectively, may therefore be especially important in the case of the strongly elongated traps used in current experiments, which have rather high radial trapping frequencies ω_x and ω_y. Therefore this kind of quantum effect should be studied in more detail. In the case of collective modes, this could be done, e.g., by comparing systematically the results obtained in quantum-mechanical quasiparticle random-phase approximation calculations [24] with those of hydrodynamics.

ACKNOWLEDGMENTS

I thank P. Schuck for fruitful discussions and critical reading of the manuscript. I also acknowledge useful discussions with S. Sinha.

[1] M. Bartenstein *et al.*, Phys. Rev. Lett. **92**, 203201 (2004).
[2] J. Kinast, S. L. Hemmer, M. E. Gehm, A. Turlapov, and J. E. Thomas, Phys. Rev. Lett. **92**, 150402 (2004).
[3] M. Cozzini and S. Stringari, Phys. Rev. Lett. **91**, 070401 (2003).
[4] M. Farine, P. Schuck, and X. Viñas, Phys. Rev. A **62**, 013608 (2000).
[5] A. Minguzzi and M. P. Tosi, Phys. Rev. A **63**, 023609 (2001).
[6] F. Zambelli and S. Stringari, Phys. Rev. A **63**, 033602 (2001).
[7] C. Menotti, P. Pedri, and S. Stringari, Phys. Rev. Lett. **89**, 250402 (2002).
[8] S. Stringari, Europhys. Lett. **65**, 749 (2004).
[9] M. Urban and P. Schuck, Phys. Rev. A **67**, 033611 (2003).
[10] A. J. Leggett, Phys. Rev. **140**, A1869 (1965); Phys. Rev. **147**, 119 (1966).
[11] O. Betbeder-Matibet and P. Nozières, Ann. Phys. (N.Y.) **51**, 392 (1969).
[12] J. R. Schrieffer, *Theory of Superconductivity* (Benjamin, New York, 1964).
[13] G. M. Bruun and H. Heiselberg, Phys. Rev. A **65**, 053407

(2002); H. Heiselberg, *ibid.* **68**, 053616 (2003).
[14] N. Nygaard, Ph.D. thesis, University of Maryland, 2004.
[15] A. Perali, P. Pieri, L. Pisani, and G. C. Strinati, Phys. Rev. Lett. **92**, 220404 (2004).
[16] K. Taruishi and P. Schuck, Z. Phys. A **342**, 397 (1992).
[17] A. L. Fetter and J. D. Walecka, *Quantum Theory of Many-Particle Systems* (McGraw-Hill, New York, 1971).
[18] G. Bruun, Y. Castin, R. Dum, and K. Burnett, Eur. Phys. J. D **7**, 433 (1999).
[19] M. Grasso and M. Urban, Phys. Rev. A **68**, 033610 (2003).
[20] M. Houbiers, R. Ferwerda, H. T. C. Stoof, W. I. McAlexander, C. A. Sackett, and R. G. Hulet, Phys. Rev. A **56**, 4864 (1997).
[21] M. A. Baranov and D. S. Petrov, Phys. Rev. A **58**, R801 (1998).
[22] M. Grasso, M. Urban, and X. Viñas, Phys. Rev. A **71**, 013603 (2005).
[23] D. Vollhardt and P. Wölfle, *The Superfluid Phases of Helium 3* (Taylor & Francis, London, 1990)
[24] G. M. Bruun and B. R. Mottelson, Phys. Rev. Lett. **87**, 270403 (2001).